

RESEARCH ARTICLE | MARCH 18 2024

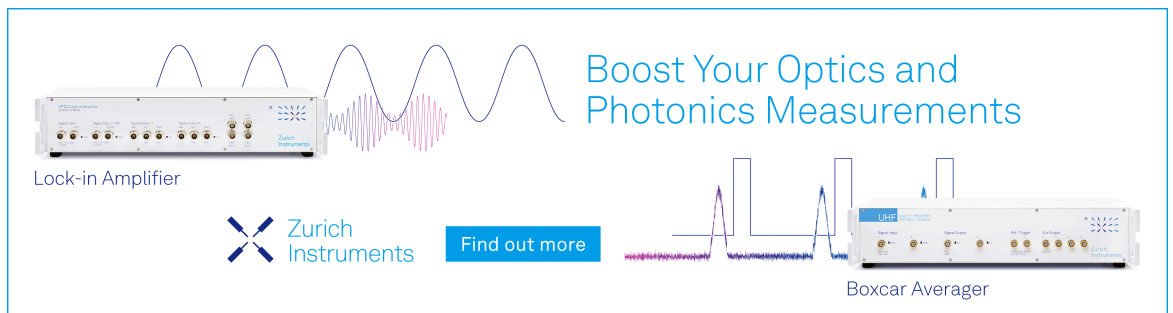
A field programmable gate array based Langmuir probe system for measurement of plasma parameters at 500 kHz in a high-power impulse magnetron sputtering plasma

C. J. Hickling   ; S. Hall  ; J. R. Harrison  ; R. Sharples  ; J. W. Bradley 



Rev. Sci. Instrum. 95, 033503 (2024)

<https://doi.org/10.1063/5.0174458>



Boost Your Optics and Photonics Measurements

Lock-in Amplifier

Zurich Instruments

Find out more

Boxcar Averager

A field programmable gate array based Langmuir probe system for measurement of plasma parameters at 500 kHz in a high-power impulse magnetron sputtering plasma

Cite as: Rev. Sci. Instrum. 95, 033503 (2024); doi: 10.1063/5.0174458

Submitted: 31 August 2023 • Accepted: 12 February 2024 •

Published Online: 18 March 2024



View Online



Export Citation



CrossMark

C. J. Hickling,^{1,2,a)}  S. Hall,²  J. R. Harrison,²  R. Sharples,³  and J. W. Bradley¹ 

AFFILIATIONS

¹Department of Electrical Engineering and Electronics, University of Liverpool, Brownlow Hill, Liverpool L69 3GJ, United Kingdom

²UK Atomic Energy Authority, Culham Science Centre, Abingdon, Oxfordshire OX14 3DB, United Kingdom

³Department of Physics, Durham University, Lower Mountjoy, South Road, Durham DH1 3LE, United Kingdom

^{a)}Author to whom correspondence should be addressed: chris.hickling@ukaea.uk

ABSTRACT

By utilizing Field Programmable Gate Arrays in a configuration similar to that of the Mirror Langmuir Probe, it is possible to bias a single probe at three precise voltages in sequence. These voltages can be dynamically adjusted in real-time based on the measured plasma electron temperature to ensure the transition region is always sampled. The first results have been obtained by employing this method and have generated real-time outputs of electron temperature, ion saturation current, and floating potential on a low temperature pulsed-DC magnetron at 500 kHz. These results are in good agreement with the analysis of a conventionally swept Langmuir probe. This probe is designed with the intention of being implemented on MAST-U to aid in the study of exhaust physics and enable further investigation into filamentary behavior.

© 2024 Author(s). All article content, except where otherwise noted, is licensed under a Creative Commons Attribution (CC BY) license (<http://creativecommons.org/licenses/by/4.0/>). <https://doi.org/10.1063/5.0174458>

I. INTRODUCTION

The benefits offered by probes are extensive, as they provide important information about the plasma they are in contact with while also being low cost and simple to operate. Conventional Langmuir probes are powerful diagnostics for measuring plasma electron temperature, ion saturation current, and floating potential and are widely used to diagnose the Scrape-Off Layer (SOL) and divertor of magnetic confinement fusion devices. Plasma in these regions is known to contain fast moving filamentary structures¹ that require highly resolved measurements (typically in the order of 100 kHz in time and 1 mm in space) to fully characterize. A triple probe provides real-time voltage dependent currents at the cost of sampling different regions of plasma. Since the triple probe samples at three constant voltage levels, it does not account for any change in temperature in the system. Conversely, a single probe provides high spatial

resolution at the cost of the time required to sweep the power supply, which also induces currents in the cables, limiting the temporal resolution, typically to the order of 10 kHz. The limitations of these conventional probes prevent fast events such as filaments from being observed.

When a probe is subjected to a bias voltage, V_B , the current in the transition region, I , can be obtained from an idealized plasma with Maxwellian electrons in a 1-D planar geometry,

$$I(V_B) = I_{sat} \left(\exp \left[\frac{e(V_B - V_f)}{k_B T_e} \right] - 1 \right). \quad (1)$$

The current, I , that is drawn by the probe depends on, the ion saturation current, I_{sat} , the floating potential, V_f , the electron temperature, T_e , and the Boltzmann constant, k_B .

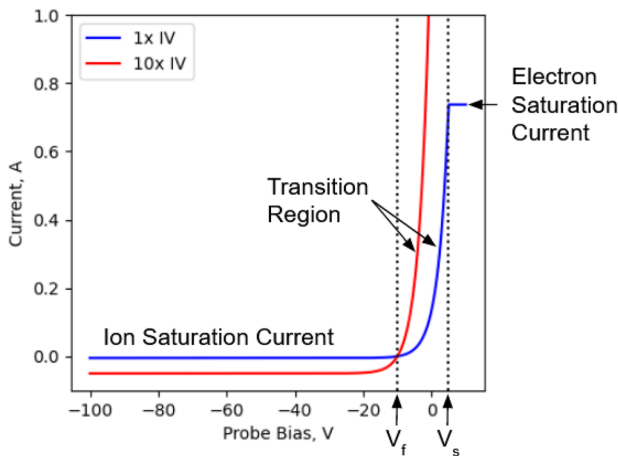


FIG. 1. A plot showing an idealized probe characteristic where V_f is the floating potential and V_s is the plasma potential. The red curve's current has been multiplied by 10 to show the ion current.

Hence, it can be seen in Fig. 1 that by sweeping a large bias voltage range, all the information needed to solve for each plasma parameter can be obtained.

Conventionally, this bias range is typically 50–100 V, and the obtained current range is defined by the density and temperature of the plasma and the collection area of the probe given by

$$I_{sat}^+ \approx \frac{1}{2} A e n_0 \left(\frac{k_b (T_e + T_i)}{m_i} \right)^{1/2}, \quad (2)$$

where n_e is the electron density of the plasma, A is the collecting area of the probe, k_b is the Boltzmann constant, T_i is the ion temperature, and m_i is the mass of the ions in the plasma. Equation (2) can be used as a close approximation of the density by assuming $T_i = T_e$ since the correction factor is small. If information regarding electron temperature is desired, time resolution is limited due to the need to sample the transition region. For this reason, probes are often used for tracking slow moving turbulence or time-averaged background plasma parameters.

Another method is to capacitively decouple the power supply from the probe and apply a high-frequency bias voltage to a single probe, which is performed in a mirror Langmuir probe implementation.² This has the advantages of both methods, but at a cost to the overall complexity of the system, coupled with an inherent reduction in the accuracy of the fit. The aim of this paper is to present a probe that can be biased sufficiently quickly to measure high speed plasma fluctuations without the complexity of the mirror probe brought about by its use of precise electrical circuits.

Previous work^{3,4} has found the Field Programmable Gate Arrays (FPGA) to be an effective tool for solving Eq. (1) with sufficient speeds to trace a slow moving 10 Hz change in the magnetic field. However, this design also presented an 80 μ s delay that would prohibit the tracking of fast events.

II. ULTRA-FAST LANGMUIR PROBE (UFLP)

A. Digital MLP algorithm

Analyzing an ideal Langmuir IV curve, it can be said that it can be divided into three regions: ion saturation, electron saturation, and transition. By assuming quasi-neutrality, all desired information can be collected without considering the electron saturation region. Hence, Eq. (1) can be solved with data points that are close to and on either side of the floating potential. By rearranging Eq. (1) for each of the three parameters of interest,

$$I_{sat} = \frac{I_{LP}}{\exp\left[\frac{e(V_B - V_f)}{k_B T_e}\right] - 1}, \quad (3)$$

$$T_e = \frac{V_B - V_f}{\ln\left(\frac{I_{LP}}{I_{sat}} + 1\right)}, \quad (4)$$

$$V_f = V_B - T_e \cdot \ln\left(\frac{I_{LP}}{I_{sat}} + 1\right). \quad (5)$$

By using a capacitor to decouple the power supply from the probe, the probe is forced to float at the floating potential as long as the time averaged current from the change in floating potential through the capacitor is zero. A capacitor is chosen such that it is sufficiently large to not attenuate the bias and draw enough current to the probe but sufficiently small to still respond to quick changes in the floating potential. Assuming both of these criteria hold true, the bias at the probe, V_B , will be the sum of the applied bias, V_A , and the floating potential, V_f ,

$$V_B = V_A + V_f, \quad (6)$$

where V_A is a positive, negative, or zero voltage with respect to the power supply's ground. These voltages are defined as V_+ , V_- , or V_0 , respectively.

In order to correctly sample the positive and negative states, the difference between the minimum and maximum applied voltages should exceed $3 \cdot k_B T_e / e$.⁵ Given that all of the information needed to estimate T_e is contained within the transition region, it is not helpful to collect an electron current greater than the magnitude of I_{sat} . By collecting the same magnitude of current in both the positive and negative bias states, there is no risk of current attenuation due to capacitor reactance.⁶

By choosing the I_{sat} to be $\pm 0.964 03 \cdot I(V_B)$ as concluded by Lyons² and solving Eq. (1) with $V_B = V_{-,+,0} + V_f$, where $V_{-,+,0} = x \cdot T_e$, thereby, giving the equations

$$\ln(-0.964 03/1 + 1) = -3.325, \quad (7)$$

$$\ln(0.964 03/1 + 1) = 0.67. \quad (8)$$

These constants can be used to choose the applied bias to the probe, as seen in Fig. 2(a). If the system is successfully decoupled, these biases should float at the floating potential of the plasma, as illustrated in Fig. 2(b).

The FPGA, a Red Pitaya Development board,⁷ is configured to take inputs of measured current and voltage and solve Eqs. (3)–(5) sequentially. Feedback controls are used to set new bias values based

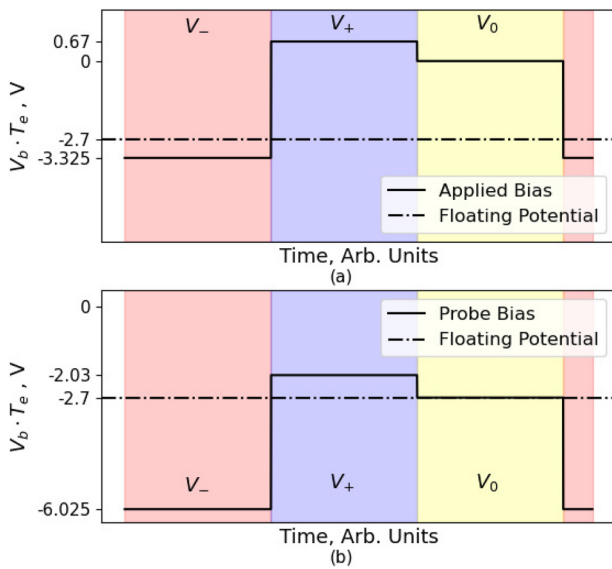


FIG. 2. A plot of the typical probe voltage bias waveform highlighting the difference between the applied bias (a) from the power supply and the probe bias (b). The probe bias is the voltage measured at the probe when the probe is capacitively decoupled in a plasma that has a floating potential of -2.7 V and an electron temperature of 1 eV.

on temperature to ensure that the transition region is always sampled. Feedback also allows the selection of the desired capacitor to maximize floating potential response time while not attenuating current.

In order to have control over the precision and precise number of clock cycles a division takes, a Goldschmidt⁸ algorithm was implemented into each of the calculation cores to solve the division. Once a valid division has been obtained, the value is input into a look-up table to return the result of the exponential in Eq. (3) and the natural logarithm in Eqs. (4) and (5). Overall, this results in a theoretical data output of 947 kHz for a completed dataset containing all three parameters, with 28 clock cycles being used for the division and 14 clock cycles for the remaining pipe-lined operations. This means that with a higher frequency clock, higher speeds could be achieved for the algorithm.

B. Capacitor switching circuit

Capacitors effectively act as frequency filters for signals. The signal that needs to be filtered away is the floating potential measured at the probe, which should vary on a time scale much less than the frequency of the applied bias to the probe. This works because capacitors have a reactance that is dependent on the value of the capacitor and the frequency of the signal, as described in the following equation:

$$X_c = \frac{1}{2\pi fC}, \quad (9)$$

where f is the applied frequency and C is the capacitance. One can see from the equation that if the frequency or capacitance decreases,

the reactance increases, attenuating the signal operating at that frequency. The aim of this circuit is to have a low reactance to the applied signal but a high reactance to the change in floating potential. This reactance also dictates the maximum amount of current that can flow through the capacitor. Since the amount of current is a fundamental property of the size of the probe and the plasma it is exposed to, this becomes an optimization between the two cases.

For this reason, a capacitor switching bank consisting of a binary switching circuit capable of a maximum of 100 nF with a resolution of 0.64 nF has been built. This is operated by GPIO pins connected directly to the Red Pitaya. These general-purpose input/output (GPIO) pins power an array of W117SIP-1 Reed Relays, which have a response time of $\sim 100 \mu\text{s}$. A look-up table is used to calibrate a measured current value in the negative bias state for a particular capacitor configuration. This allows a total of 128 different combinations of capacitor values. This is an improvement over the original Mirror Langmuir Probe (MLP) circuit, which only had eight different capacitor thresholds.

C. AC coupling compensation

In order to address the delay seen by McCarthy,⁴ the system must further build on the assumption of the capacitor successfully decoupling from the plasma. In the event of an overestimate of applied temperature, the assumption of net zero current through the capacitor breaks down. This is because the current in the positive state has a greater magnitude than in the negative state. This causes an AC coupling offset equal to the time averaged current, as illustrated in Fig. 3. This not only causes the parameters to be inaccurate but also greatly increases convergence time as the floating potential and ion saturation current are no longer small corrections. This can be digitally removed by sampling the current in the zero state and mathematically subtracting it on each iteration. This has reduced the delay in the convergence time of the algorithm down to a single operation cycle. In the case of the results of this paper, that equates to $2 \mu\text{s}$.

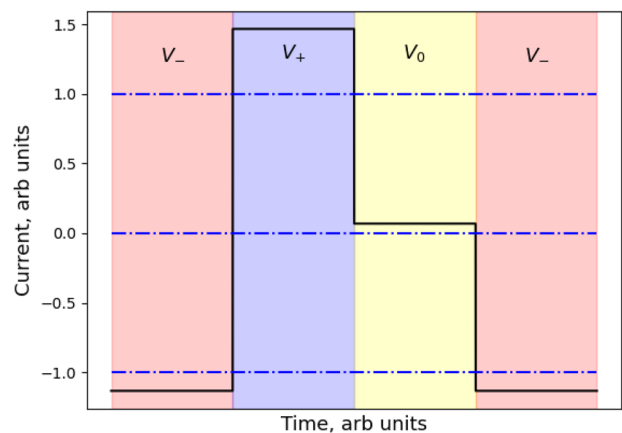


FIG. 3. Figure of the relationship between the measured current in each of the three states when an overestimated temperature is used in the applied bias states when the circuit is capacitively coupled to a power supply causing AC coupling.

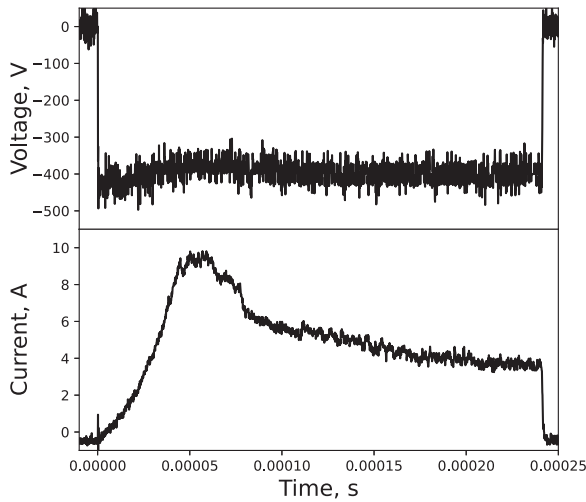


FIG. 4. A plot of the discharge voltage and current from the HiPIMS drive supply lasting 250 μ s at University of Liverpool.

III. EXPERIMENTAL SETUP

A. The plasma system

The plasma source used in this study is a planar magnetron used for the deposition of engineering quality thin films. It consists of an electrically conductive target plate that is often water cooled, behind which sits a permanent magnet. Above the target are a number of closed magnetic field lines, which form what is known as a “magnetic trap.” By driving the target plate with a large current, as seen in Fig. 4, plasma can be formed.

Densities up to 10^{19} m^{-3} can be achieved within the magnetic trap with typical electron temperatures, T_e , of 2–5 eV. The confined

plasma has a broad spectrum of plasma waves and instabilities in the frequency range of kHz to MHz.⁹ By operating a magnetron with a high-power impulse magnetron sputtering (HiPIMS) power supply, the resulting plasma has a well-defined profile^{10,11} with a short pulse length that has similar plasma parameters to the divertor or scrape-off layer of a tokamak.

Power is supplied to the magnetron source via one of two different power sources. This can either be an advanced energy, Pinnacle 18 kW supply, which can be operated in either a DC mode or a pulsed DC mode with a minimum frequency of 5 kHz and a minimum off time of 5 μ s at this frequency. The device can also be powered by an in-house custom built HiPIMS power supply unit, which is described in detail in Ref. 10. The voltage and current of both of these power supplies pass through a junction box, where the voltage and current are measured by a Tektronix P5 100 voltmeter and a Pearson 3972 current monitor, respectively. These are connected to a Tektronix DPO 3034 oscilloscope for monitoring the power to the target plate.

B. Data acquisition system

The experimental setup, detailing a Red Pitaya, amplifier and plasma system, is seen in Fig. 5.

The drive signal is generated by the Red Pitaya. Immediately following a reset state, the device initializes some guesses about the requested parameters. The initial temperature guess is used to generate the very first bias output. From here, each completed cycle will hone the bias range based on the new temperature values that are calculated. The Red Pitaya has the capability to output a 125 MHz signal in the voltage range of ± 1 V. In order to sample low temperature plasmas, an HS-401 bipolar amplifier has been used to supply a gain of 20 to the original signal. The voltage is measured directly via a voltage probe into the analog-to-digital converter (ADC) (± 20 V) on the Red Pitaya. The current needs to first be isolated from the main path via the use of a 1:1 isolation transformer before measuring the

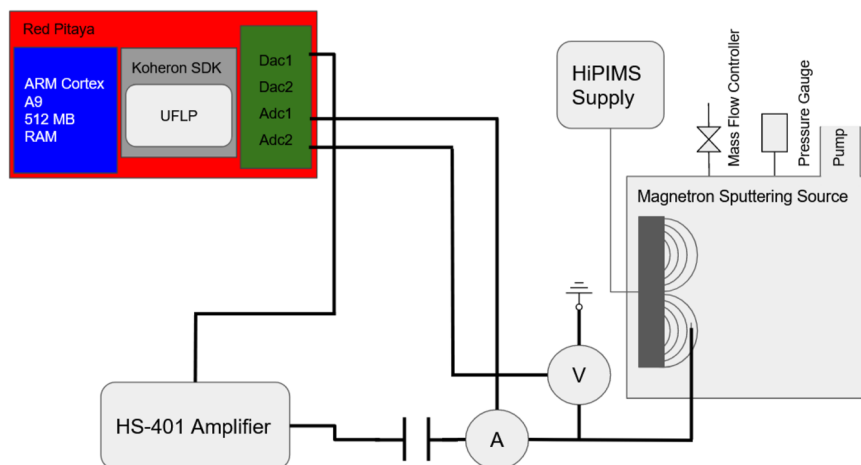


FIG. 5. A schematic of the experimental setup of a HiPIMS driven magnetron operating with an argon plasma at 12 mTorr of gas pressure. HiPIMS settings at 50 Hz repetition rate with 250 μ s on time.

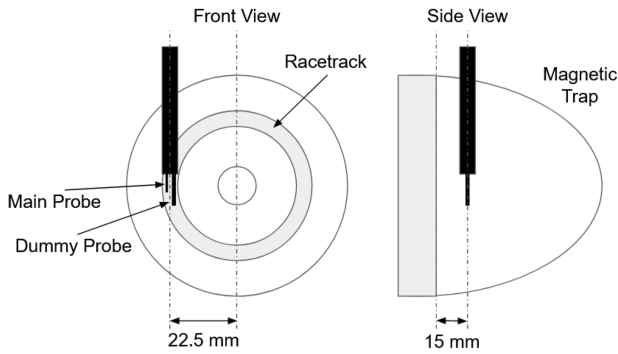


FIG. 6. Diagram illustrating the position of the probes relative to the magnetron target plate.

C. Langmuir probe configuration

The Langmuir probe used is a 0.25 mm radius tungsten wire tip that is 10 mm in length. There is an identical probe that exists as a coiled pair, next to the main probe, that is completely shielded from the plasma using a ceramic tube coating. This is used to compensate for the stray capacitance induced by the high frequency switching bias. The main probe is also capable of being used as a regular Langmuir probe by connecting it to an Impedans ALP-1000. This is an off-the-shelf trigger enabled Langmuir probe analysis tool that, when connected to a probe, can perform a configured voltage sweep and measure the current. Since it can be triggered by a signal, it can be connected to the trigger signal of the HiPIMS pulse, which is produced by the University of Liverpool's in-house kick pulse generator. This allows the ALP-1000 to make use of a delay generator to measure each part of the pulse with the desired voltage to form an IV curve for each part of the pulse over many cycles. This raw current and voltage data are then saved and analyzed in Python to return floating potential, ion saturation flux, electron temperature, and electron density.

The position of the probe in all cases is ~ 15 mm from the target plate positioned above the racetrack, as detailed in

voltage on both sides of a sense resistor. In the case of a HiPIMS measurement, this voltage needs to be stepped down to be within the rail voltage of the instrumentation amplifier used to calculate the current. A gain resistor is used to set the input to $1\text{ V} = 7\text{ mA}$.

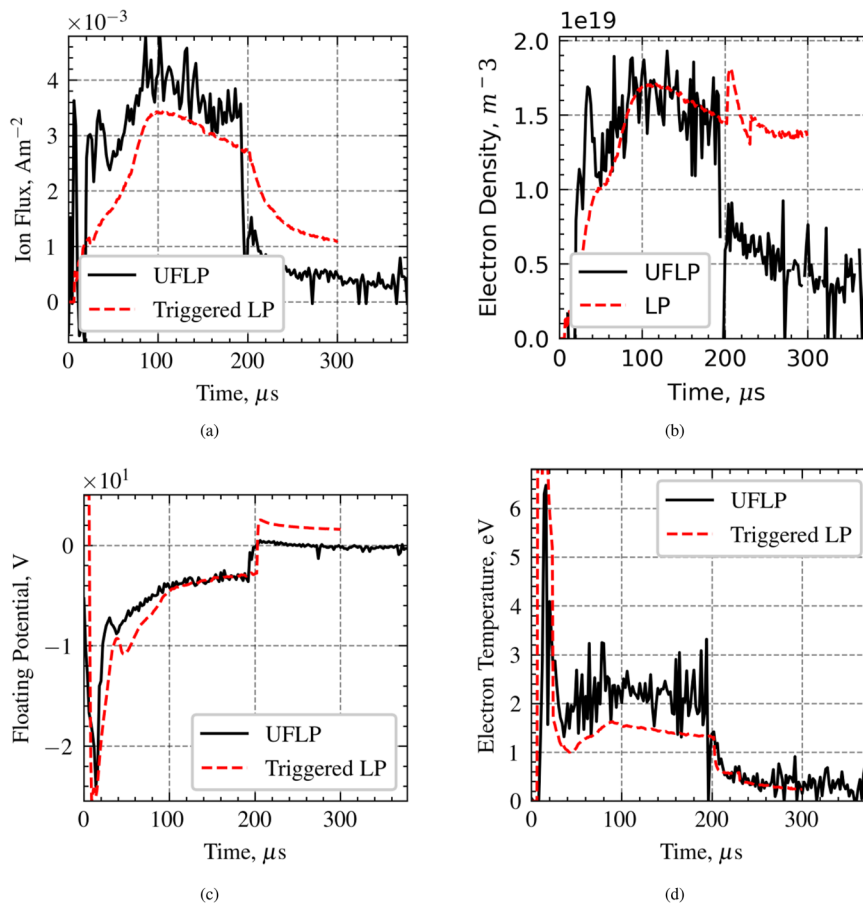


FIG. 7. Ion flux (a), plasma density (b), floating potential (c), and electron temperature (d) gathered at 500 kHz using a single probe multiplexed at dynamic bias at values of $V_{+,-,0} = 0.64\text{ TeV}, -3.325\text{ TeV},$ and 0 V .

15 May 2024 08:51:04

Fig. 6. This is to maximize density for larger currents into the probe.

The position of the dummy probe relative to the main probe should be negligible, as following the same path is mostly to ensure it is exposed to the same electromagnetic fields and is the same length rather than in the same plasma. This holds true as long as the sheaths of the two probes do not intersect.

IV. RESULTS

Results can be seen in **Fig. 7** for the Ultra-Fast Langmuir Probe (UFLP)¹³ compared to a conventionally swept method. The UFLP successfully starts from a pre-programmed initial guess and quickly converges to a solution that closely matches the results given by a triggered conventional Langmuir probe system. It can be seen that the delay seen in McCarthy⁴ is significantly reduced by the modifications applied to the processing method. This allows the UFLP to successfully lock on to a signal that is only 200 μs in full duration, in 2 μs , and the shape of the pulse is tracked to high fidelity. There is an apparent offset error in the current and, consequently, the temperature, likely due to an insufficient decoupling effect of the capacitor (which changes faster than an individual calculation cycle). There is also disagreement on the density of the plasma at the end of the HiPIMS pulse. This is likely due to the UFLP gathering data for a single pulse in comparison to the ALP-1000's average data of 11 000 pulses. The duration of the current supplied by a HiPIMS pulse can vary by as much as $\pm 20 \mu\text{s}$. In addition, in this region, the ion and electron temperatures will be vastly different.

The UFLP is capable of replicating the functionality of a triggered Langmuir probe in real time with a data output rate of 500 kHz. This is a frequency at which some interesting plasma phenomena exist in HiPIMS plasmas such as spokes.¹⁰ The noise seen in **Fig. 7** could be an artifact of such plasma phenomena, but it has little to no frequency dependence. This is likely due to the proximity of the data sample rate to the Nyquist frequency of the turbulence.

V. CONCLUSIONS

Building on previous work, high speed plasma fluctuations have been measured in a low temperature HiPIMS system at 500 kHz using this technique, as shown in **Fig. 7**. Dynamic voltage switching has also been implemented to adjust the bias range to changing temperatures. The acquisition speed was limited to 500 kHz due to bandwidth limitations in the current measurement, but hardware simulations suggest 947 kHz is achievable with the given FPGA design. Simulations and analysis of previous data¹² have also confirmed that 500 kHz is likely sufficient for observing filaments in the MAST-U tokamak. These preliminary tests prove the efficacy of this diagnostic to enable the study of fast filamentary structures.

ACKNOWLEDGMENTS

The authors would like to acknowledge Dr. William McCarthy and Dr. Theodore Golfopoulos at the MIT Plasma Science and Fusion Center, as well as Dr. Charles Vincent and Dr. Jack Lovell

at UKAEA, for their invaluable insight and assistance in this work. This work has been funded by the RCUK Energy Program (Grant No. EP/T012250/1) and supported by the Engineering and Physical Sciences Research Council (Grant No. EP/L01663X/1). This work was planned to be continued by a Ph.D. student starting at the University of Liverpool, collaborating with UKAEA. The ability of this new diagnostic to operate at extremely high frequencies will provide an exciting incite into filamentary behavior on MAST-U.

AUTHOR DECLARATIONS

Conflict of Interest

The authors have no conflicts to disclose.

Author Contributions

C. J. Hickling: Conceptualization (equal); Data curation (lead); Formal analysis (lead); Investigation (equal); Methodology (lead); Software (lead); Writing – original draft (lead); Writing – review & editing (lead). **S. Hall:** Conceptualization (equal); Resources (equal); Supervision (equal). **J. R. Harrison:** Conceptualization (equal); Resources (equal); Supervision (equal). **R. Sharples:** Conceptualization (equal); Supervision (equal). **J. W. Bradley:** Conceptualization (equal); Investigation (equal); Project administration (lead); Resources (equal); Supervision (equal).

DATA AVAILABILITY

The data that support the findings of this study are available from the corresponding author upon reasonable request.

REFERENCES

- ¹N. Walkden, F. Riva, J. Harrison, F. Militello, T. Farley, J. Omotani, and B. Lipschultz, "The physics of turbulence localised to the tokamak divertor volume," *Commun. Phys.* **5**, 139 (2022).
- ²B. Labombard and L. Lyons, "Mirror Langmuir probe: A technique for real-time measurement of magnetized plasma conditions using a single Langmuir electrode," *Rev. Sci. Instrum.* **78**, 073501 (2007).
- ³C. Vincent, W. McCarthy, T. Golfopoulos, B. LaBombard, R. Sharples, J. Lovell, G. Naylor, S. Hall, J. Harrison, and A. Q. Kuang, "The digital mirror Langmuir probe: Field programmable gate array implementation of real-time Langmuir probe biasing," *Rev. Sci. Instrum.* **90**, 083504 (2019).
- ⁴W. McCarthy, T. Golfopoulos, K. B. Woller, C. Vincent, A. Kuang, and B. Labombard, "First application of a digital mirror Langmuir probe for real-time plasma diagnosis," *Rev. Sci. Instrum.* **92**, 103502 (2021).
- ⁵P. C. Stangeby, *The Plasma Boundary of Magnetic Fusion Devices* (Institute of Physics Publishing, 2000), p. 717.
- ⁶L. A. Lyons, "Construction and operation of a mirror Langmuir probe diagnostic for the Alcator C-Mod tokamak," Massachusetts Institute of Technology, 2005, http://dspace.mit.edu/bitstream/handle/1721.1/93288/07rr008_full.pdf.
- ⁷P. Leban, Red pitaya user manual, 2014, <http://docs-asia.electrocomponents.com/webdocs/144a/0900766b8144a693.pdf> (accessed 09 September 2019).
- ⁸R. E. Goldschmidt, "Applications of division by convergence," Ph.D. thesis, Massachusetts Institute of Technology, Boston, 1964.
- ⁹F. Lockwood Estrin, S. Karkari, and J. W. Bradley, "Triple probe interrogation of spokes in a HiPIMS discharge," *J. Phys. D: Appl. Phys.* **50**, 295201 (2017).

¹⁰P. Poolcharuansin and J. W. Bradley, “Short- and long-term plasma phenomena in a HiPIMS discharge,” *Plasma Sources Sci. Technol.* **19**, 025010 (2010).

¹¹F. L. Estrin, “The study of spokes in HiPIMS discharges with applications to the production of superconducting thin films,” Ph.D. thesis, University of Liverpool, 2016, <https://core.ac.uk/reader/131164120>.

¹²D. A. D’ippolito, J. R. Myra, and S. J. Zweben, “Convective transport by intermittent blob-filaments: Comparison of theory and experiment,” *Phys. Plasmas* **18**, 60501 (2011).

¹³C. Hickling (2023). All code can be found in Git repository. <https://gitlab.com/chickling1994/uflp>